

# Estimating the Molten Salt Flow Rate for the MSRE Isothermal Transient Benchmark Development

Mohamed Elhareef and Zeyun Wu

Department of Mechanical and Nuclear Engineering, Virginia Commonwealth University, Richmond VA 23284  
[elhareefmh@vcu.edu](mailto:elhareefmh@vcu.edu); [zwu@vcu.edu](mailto:zwu@vcu.edu)

## INTRODUCTION

Molten Salt Reactor (MSR) is a Gen IV [1] reactor concept where the fissile materials are dissolved in a molten salt mixture acting as both fuel and coolant in the primary loop of the reactor. The fuel flowing nature gives the MSR design several advantages including online refueling, processing, and fission product removal; high coolant outlet temperature; low operating pressure; and inherent safety characteristics [2]. However, the drift of delayed neutron precursors (DNPs) and fission products outside the MSR core with the coolant flow makes a strong coupling between the neutronics and thermal hydraulics phenomena in such systems. As a result, the development of computational tools for simulating MSR systems requires high-quality data for code validation. The Molten Salt Reactor Experiment (MSRE) performed in the 1960s [3] is currently the only reliable experimental data source for this class of reactors. The MSRE is a 10 MW thermal reactor that was moderated by graphite and cooled by a FLiBe salt mixture. During the operational period of the MSRE several transient experiments were conducted.

A series of MSRE flow transient tests were conducted to serve the following goals [4]: obtain the fuel pump and coolant pump startup and coastdown characteristics; infer fuel salt flow rate characteristics during coast down; determine transient effects of fuel flow rate changes on reactivity. The MSRE flow rate transient tests were conducted at zero power with the absence of circulating voids [4]. During these transient tests, a flux servo controller was used to ensure the reactor be operated at critical status. The reactivity change due to flow perturbation was then measured from the reactivity added by control rods. Under these conditions, the reactivity changes are attributed entirely to be the flow effects on delayed neutron precursors [5].

During the flow transient tests, both the fuel pump speed and coolant pump speed were recorded in the pump startup and pump coastdown test. But only the flow rate in the coolant salt loop (i.e., the second loop) was recorded [5]. The flow rate in the fuel salt loop (i.e., the primary loop) is missing. The test results showed that the coolant pump speed and coolant flow rates are not in unison. Thus, this pump speed data cannot directly be used to infer the flow rate in the fuel loop. An attempt to generate the undocumented fuel pump transient characteristics were made in ref. [6]. An analytical method combined with the steady-state pump curve were used to estimate the pump head as a function of time for both the pump startup and pump coastdown tests.

In this work, a pump transient model to estimate the transient flow rate in the primary loop is developed. This approach leverages the recorded data in the secondary loop and the similarity of the two MSRE pumps to reconstruct the homologous pump head.

## MSRE FLOW TRANSIENT OVERVIEW

The MSRE fuel circulation loop, depicted in Fig. 1, consists of the reactor vessel, fuel pump, primary heat exchanger, and piping system. The fuel salt enters the cylindrical reactor vessel through an annular volute around the top of the cylinder and flows downwards between the vessel and the graphite matrix. A dished head at the bottom forces the flow in the upward direction through rectangular passages in the graphite matrix to the top head. The fuel then flows the suction line of the primary pump and then discharge to the shell side of a U-tube heat exchanger. Fuel pump is sump-type centrifugal pump rotates at 1160 rpm delivers 1200 gpm ( $0.076 \text{ m}^3/\text{s}$ ) at 49 ft ( $\sim 15\text{m}$ ) of fluid [3]. The heat exchanger (HX) is designed for heat load of 10 MW. The pipe size is 5 inch, and the flow speed at 1200 gpm is 20 ft/s ( $\sim 6\text{m/s}$ ). The total volume of the fuel salt in the primary loop is  $73 \text{ ft}^3$  ( $\sim 2\text{m}^3$ ) [3].

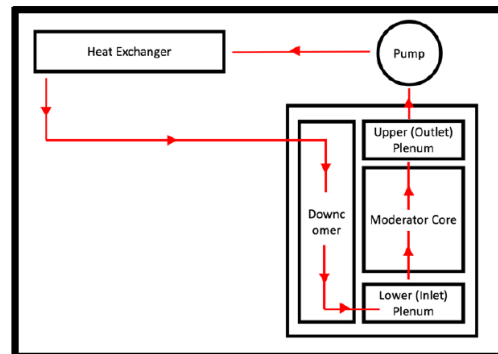


Fig. 1. A schematic view of the primary loop of MSRE.

The coolant salt in the second loop, depicted in Fig. 2, is circulated in the tube side in the HEX and then travels to the suction line of the coolant pump before it dissipates heat to air through the radiator. The tube side of the HEX consists of 159 U-tubes of  $\frac{1}{2}$ -in OD. The radiator consists of 120 tubes of  $\frac{3}{4}$ -in OD. The coolant pump rotates at 1750 rpm to deliver 850 gpm ( $0.05 \text{ m}^3/\text{s}$ ) of salt against 78 ft ( $\sim 24\text{m}$ ) head [3]. The salt volume in the secondary loop is about  $45 \text{ ft}^3$  ( $\sim 1.3\text{m}^3$ ).

The pump startup and pump coastdown tests are conducted at zero power (~10 watts). The power was kept constant during the transients by adjusting the fuel rod position inside the core. During the pump startup test, the pump speed was increased linearly from zero to 100% in 1 s then it was kept constant during the transient [5]. In the pump coast down test, starting from steady state flowing conditions, the pump motor was turned off. All the recorded pump speeds and the flow rate in the secondary loop during the flow transients can be found in ref. [5]. The change in the control rod position during the pump transient tests can be found in ref. [4].

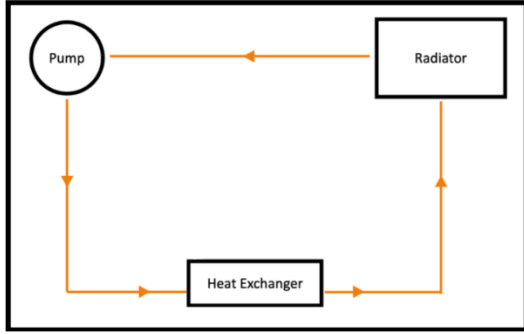


Fig. 2. A schematic view of the second loop of MSRE.

## COMPUTATIONAL MODELS

A quasi-1D, fully neutronics/thermal hydraulics (N/TH) coupled model has been developed to describe the MSRE flow transients. The system consists of a two-energy group neutron diffusion model, a six-family DNP drift model, and the mass and momentum conservation models of the fuel salt. With standard notations for nuclear reactor analysis, the system of equations of the N/TH model is given by

$$\begin{aligned} \frac{1}{v_1} \frac{\partial \phi_1}{\partial t} - \frac{\partial}{\partial z} D_1 \frac{\partial \phi_1}{\partial z} + \Sigma_{r1} \phi_1 &= (1 - \beta) \sum_g \nu \Sigma_{fg} \phi_g + \sum_{k=1}^6 \lambda_k C_k, \\ \frac{1}{v_2} \frac{\partial \phi_2}{\partial t} - \frac{\partial}{\partial z} D_2 \frac{\partial \phi_2}{\partial z} + \Sigma_{r2} \phi_2 &= \Sigma_{s,1 \rightarrow 2} \phi_1, \\ A \frac{\partial C_k}{\partial t} + Au \nabla_i \cdot C_k &= A \beta_i \sum_g \nu \Sigma_{fg} \phi_g - A \lambda_k C_k, \quad k = 1, \dots, 6, \\ A \frac{\partial \rho}{\partial t} + \nabla_i \cdot (A \rho u) &= 0, \\ \rho \frac{\partial u}{\partial t} + \rho u \cdot \nabla_i u &= -\nabla_i p - f_D \frac{\rho}{2d_h} |u| + F. \end{aligned} \quad (1)$$

Here  $\nabla_i$  is the gradient in the flow tangent direction. Eq.(1) is solved using COMSOL Multiphysics software [7] in this work. The neutron diffusion equations are implemented in the mathematics module while the DNP equations and the fluid dynamics equation are implemented in the Reacting Pipe Flow interface. A fully coupling between the two components is achieved by exchanging the fission source and the delayed neutron source between the two components.

For centrifugal pumps in a closed loop, the equation for the pump transient is governed by [8, 9]

$$\begin{aligned} \sum \frac{L_i}{A_i} \frac{dq}{dt} + K_{cl} \frac{q^2}{2\rho} - \rho g h_p &= 0, \\ I \frac{d\omega}{dt} &= M_{em}(\omega) - M_h(\omega) - M_f(\omega) \end{aligned} \quad (2)$$

where  $L_i, A_i$  are the length and flow area of the  $i^{\text{th}}$  section of the circulation loop,  $q$  is the mass flow rate,  $h_p$  is the pump head,  $K_{cl}$  is resistance coefficient,  $I$  is the moment of inertia of the pump,  $\omega$  is the pump angular speed,  $M_{em}, M_h$  and  $M_f$  are the electromagnetic, hydraulic, and friction torque, respectively. By assuming that the developed head  $h_p$  is proportional to the square of pump speed  $\omega$  [8, 9], the pressure drop equation in Eq. (2) can be rewritten as

$$\sum \frac{L_i}{A_i} \frac{1}{\rho g h_{p0}} \frac{dq}{dt} = \left( \frac{\omega}{\omega_0} \right)^2 - \frac{q^2}{q_0^2}. \quad (3)$$

## RESULTS

The secondary loop data is used to test the applicability of Eq. (3) for the MSRE pumps. The measured coolant pump speed during the pump startup test is used as input for the pump transient model given by Eq.(3). The model predicted flow rate compared to the measured flow rate during pump startup transient is shown in Fig. 3. As can be seen, the pump transient model was found to be sufficient for the pump startup case with Root Mean Square Error (RMSE) with the measured data of 6.0036 kg/s. The discrepancy between the model predictions and the measured data can be partially attributed to the uncertainties in the geometrical parameters of the secondary loop, the density of coolant salt and the measured pump speed and flow rate. These results confirm that the pump model described above and the underlying assumptions are appropriate for the pump startup case.

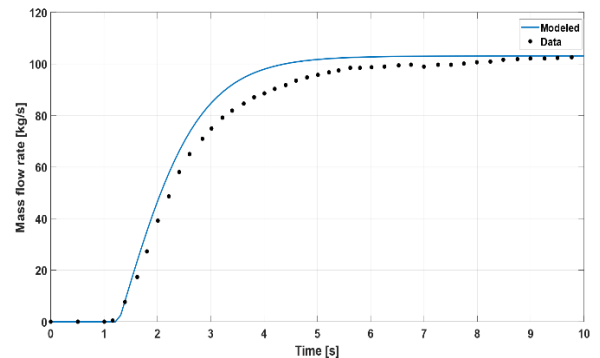


Fig. 3. The coolant flow rate during the pump startup transient estimated by Eq. (3).

Similar to the pump startup case, the measured coolant pump speed and flow rate for the pump coastdown test are also used to verify the applicability of Eq.(3) for the coastdown test. The model predicted flow rate compared to

the measured data for this case is shown in Fig. 4. As can be seen, large discrepancies were noticed between the set of data. The RMSE in the modeled flow rate is about 11.18 kg/s. A closer inspection at the flow rate profile indicates that there is a sudden reduction in the flow rate after ~5 s into the transient. This suggests that the assumption that the pump head is proportional to the square of the pump speed may not be adequate for the case of pump coastdown transient in the MSRE pump design.

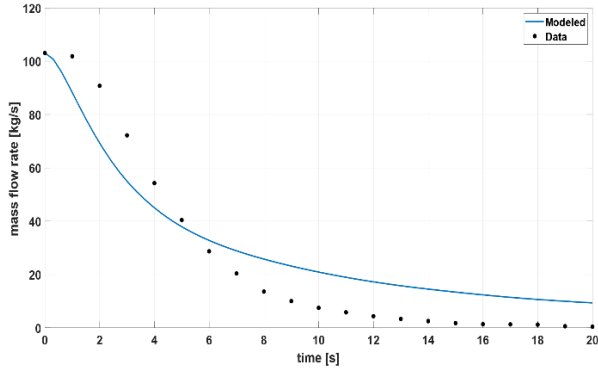


Fig. 4. The coolant flow rate during the pump coastdown transient estimated by Eq.(3).

To overcome the limitations imposed by the pump head assumption, a different approach is employed in the pump coastdown case to predict the pump flow rate. This new approach relies on reconstructing the homologous pump head characteristics using the measured data for the coolant pump. The homologous pump characteristics are used to present the pump transients [10]. The homologous pump head characteristics curve gives the relationship between the normalized pump speed ( $v$ ), normalized flow rate ( $\alpha$ ), and normalized head ( $\alpha$ ) defined as [**Error! Reference source not found.**]

$$v = \frac{N}{N_0}, \quad \alpha = \frac{Q}{Q_{ss}}, \quad h = \frac{h_p}{h_{p_0}}. \quad (4)$$

To estimate this relationship for the MSRE pump, the normalized pump hydraulic power is defined as

$$P = \frac{Qh_p}{Q_{ss}h_{p_0}} = \alpha h. \quad (5)$$

Substituting Eq. (4) & (5) into Eq. (3) results in the following ODE for estimating the pump flow rate for the primary loop.

$$\frac{1}{\rho g h_{p_0}} \sum \frac{L_i}{A_i} \frac{dq}{dt} = \frac{q_{ss}}{q} P(v) - \frac{q^2}{q_0^2}. \quad (6)$$

The measured pump speed and flow rate in the secondary loop during the pump coastdown are used to estimate the normalized head and normalized power. The functional dependence between  $P$  and  $v$  was established by means of least square error fitting.

To verify the approach, Eq.(6) is firstly solved for the coolant pump in the second loop. The flow rate results

compared to both the measured data and the solution of Eq. (3) are shown in Fig. 5. It can be seen, the model predicted flow rate during the pump coastdown case has significantly improved with the RMSE of 1.7545 kg/s.

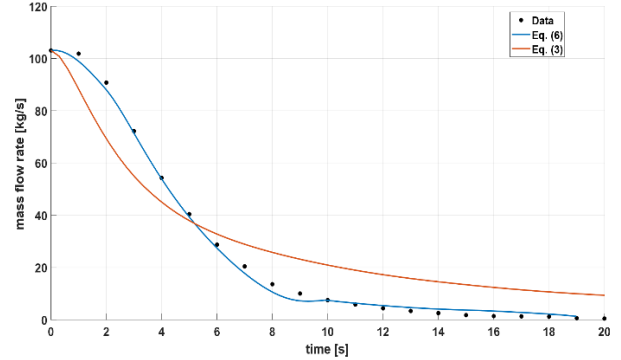


Fig. 5. The coolant flow rate during the coolant pump coastdown estimated by Eq.(6) and Eq.(3), respectively.

Based on these findings, Eq. (3) is used to obtain the flow rate in the primary loop during fuel pump startup. On the other hand, Eq. (6) will be used for the case of fuel pump coastdown. It was assumed that the two pumps (the fuel pump and coolant pump) have the same normalized hydraulic power dependence on  $v$ .

The reactivity response to the transient flow rate was estimated by weighting the fission source term in Eq. (1) to keep the power constant at 10W. This scaling factor ( $\theta$ ) is then used to estimate the inserted reactivity defined as:

$$\rho(t) = \frac{\theta_0 - \theta(t)}{\theta(t)}, \quad (7)$$

where  $\theta_0$  is the initial scaling factor, which is also the  $k$ -eigenvalue of the fundamental mode at static fuel condition.

Table I. DNP parameters for the MSRE static fuel.

| G | Set 1 [4]                |           | Set 2                    |           |
|---|--------------------------|-----------|--------------------------|-----------|
|   | $\lambda_i$ [ $s^{-1}$ ] | $\beta_i$ | $\lambda_i$ [ $s^{-1}$ ] | $\beta_i$ |
| 1 | 1.24E-02                 | 2.11E-04  | 1.25E-02                 | 2.09E-04  |
| 2 | 3.05E-02                 | 1.40E-03  | 3.18E-02                 | 1.07E-03  |
| 3 | 1.11E-01                 | 1.25E-03  | 1.09E-01                 | 1.04E-03  |
| 4 | 3.01E-01                 | 2.53E-03  | 3.17E-01                 | 2.96E-03  |
| 5 | 1.14E+00                 | 7.40E-04  | 1.35E+00                 | 8.66E-04  |
| 6 | 3.01E+00                 | 2.70E-04  | 8.64E+00                 | 3.05E-04  |

The neutron diffusion model is solved for the reactor core and the albedo boundary condition is constructed and applied to account for the axial neutron leakages. A fictitious leakage cross section is used to account for the radial neutron leakage. Six DNP families are assumed. The cross sections and albedo factors are generated using the MSRE Serpent model developed in Ref. [11]. Two different sets of DNPs parameters are tested in this work. The 1<sup>st</sup> set is from the MSRE legacy documents (Table 2. in Ref. [4]). The 2<sup>nd</sup> set

was generated using the MSRE Serpent model mentioned above. The two sets of data are listed in Table I.

The reactivity response predictions based on the two sets of data for the pump startup transient and pump coastdown transient are shown in Fig. 6 and Fig. 7, respectively. As can be seen, the two responses have shown some differences, in which the predictions based on 1<sup>st</sup> set of data have exhibited a better agreement with the measured data. The larger oscillations appeared in the simulation could be a result of not considering the gaseous fission products removal in the model.

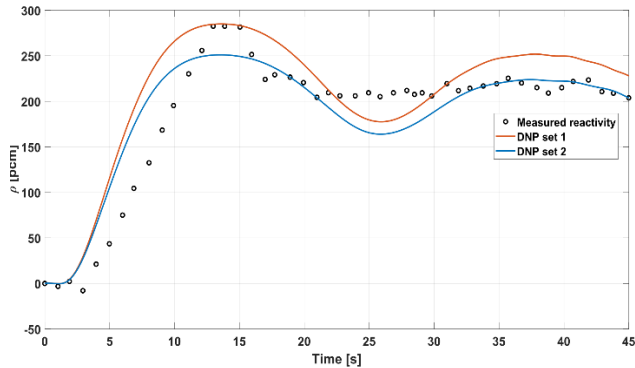


Fig. 6. The reactivity response for the pump startup.

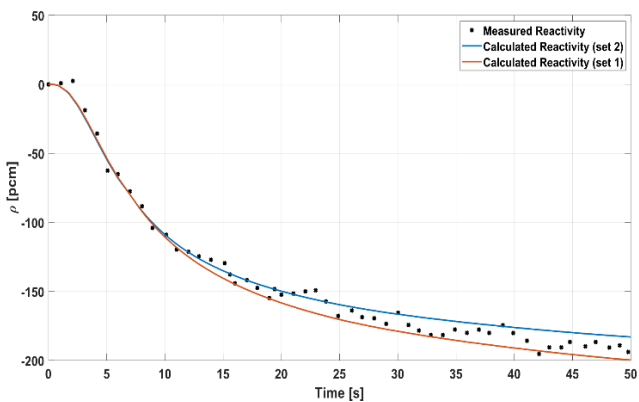


Fig. 7. The reactivity response for the pump coastdown.

For the pump startup transient, as the DNP concentration decrease inside the core, positive reactivity is then added to balance the loss of delayed neutrons. With the return of the undecayed DNPs to the core this reactivity demand decrease. This gives the solution a damped oscillation behavior with period of about 25 s, which is the salt circulation period. The simulation estimates the reactivity insertion faster than the experimental data. Moreover, the estimated reactivity shows larger oscillations compared to the experiment. However, the solution converges to the experimental data as it reaches steady state. For the pump coastdown test, the DNPs concentration inside the core increases gradually. Thus, negative reactivity is added to compensate for the extra delayed neutrons arising in the system. The experimental and simulated data are in well agreement.

## CONCLUSIONS

In this work, the undocumented transient flow rate during the MSRE pump transient tests was estimated using the measured data in the secondary loop to test the underlying assumptions of the pump transient model. It was found that during the pump startup transient, the pump head was proportional to the square of the pump speed. For the pump coastdown case, this assumption was proved to be insufficient and the homologous pump characteristics was estimated from the secondary loop data. These characteristics were assumed to be the same for both the primary and secondary pumps. A simplified neutronics and T/H coupled model of the MSRE fuel circulation loop was developed. The model was employed to analyze the fuel pump startup and coastdown transients. The estimated transient flow rate was used as input for the coupled calculations. It was demonstrated that the model successfully captured the main characteristics of the reactivity changes due to fuel circulation.

Further analysis is needed to examine the reactivity oscillations. This is planned to be conducted by modeling the gaseous fission products removal system. In the future work the model capability for non-isothermal and compressible flow conditions will be added. These models will then be used to carry out a sensitivity analysis for the MSRE parameters in order to develop a transient benchmark for MSRs modeling tools.

## ACKNOWLEDGEMENTS

We thank Prof. Massimiliano Fratoni for providing us the MSRE Serpent model to generate the neutronics parameters. We also thank Mr. Theodore Chu for the initial drawings of Fig. 1&2. This work is performed with the support of U.S. Department of Energy's Nuclear Energy University Program (NEUP) with the Award No. DE-NE0009162.

## REFERENCES

1. Gen IV International Forum - GIF, 2010 Annual Report. OECD Nuclear Energy Agency, (2010).
2. T. J. DOLAN, *Molten Salt Reactors and Thorium Energy*, Woodhead Publishing (2017).
3. R. C. ROBERTSON, ORNL-TM-728, ORNL (1965).
4. B.E. PRINCE et al., ORNL-4233, ORNL (1968).
5. R. B. BRIGGS, ORNL-3872, ORNL (1965).
6. T. FEI et al., "MSRE Transient Benchmarks using SAM," PHYSOR 2020 (2020).
7. COMSOL Multiphysics Reference Manual, (2014).
8. K. FARHADI et al., *Prog. Nucl. Energy*, **49**(7) (2007).
9. H. GAO et al., *Nucl. Eng. Design*, **241**(2) (2011).
10. J. PARK et al., *Nucl. Eng. Design*, **357**, (2020).
11. D. SHEN et al., "Reactor Physics Benchmark of the First Criticality in the Molten Salt Reactor Experiment," *Nucl. Sci. Eng.*, **195**(8) (2021).